Solitons in a macroscopic traffic model

P. Saavedra * **R. M. Velasco** **

* *Department of Mathematics, Universidad Autónoma Metropolitana, Iztapalapa, 09340 México, (e-mail: psb@xanum.uam.mx).*
** *Department of Physics, Universidad Autónoma Metropolitana, Iztapalapa, 09340 México, (e-mail: rmvb@xanum.uam.mx).*

Abstract: The steady behavior in the macroscopic Kerner and Konhäuser (1993, 1994, 1997) traffic model in a closed circuit, is studied numerically to see the time evolution of perturbations around the homogeneous steady case[9]. The simulation shows that after a transient time interval, the perturbation develops a traveling wave structure with the characteristics associated to a typical soliton in nonlinear partial differential equations. In traffic flow, the formation of solitons indicate the permanent presence of jams along the road. The solitons characteristics depend on the fundamental diagram and the specific values in the viscosity and the velocity variance introduced in the model. The nonlinearity and dissipation in the model cause the propagation of the traveling wave, Drazin (1990)[3].

Keywords: Solitons, Traffic models, Traffic jams.

1. INTRODUCTION

Traffic problems represent an actual challenge from several points of view. The practical management of traffic concerns aspects which go from the design to the control in highways. In contrast with it, there are some unsolved problems which deal with the models and their fundamental support. It is along these lines that our work may be interesting in the traffic flow literature. The macroscopic models common to traffic problems in highways have a long history, the fundamental diagram was studied by Greenshields (1935) [5] more than seventy years ago, then it has been updated with experimental data and some correlations which allow for an analytical treatment. Several models have been proposed to describe the main characteristics of traffic, and they have the advantage that their simulation under some boundary and initial conditions gives us a tool to guide our understanding. Models like the Lighthill-Whitman-Richards (1955,1956) [12] were some of the first ones to introduce continuum equations to study traffic flow based on a partial differential equation (PDE) constructed for the density. In this case the constitutive equation linking the flux with the density was introduced through the fundamental diagram and shock waves appeared in the solution, making necessary the introduction of a kind of diffusion coefficient. Some other models went in this direction as shown by Nelson (2000)[15] however it was soon recognized that the speed of vehicles must be an independent quantity. Models such as the one proposed by Payne (1971)[16], and Kühne (1993) [10] were implemented giving place to some non-physical results. Later on, the analogy between traffic flow and the compressible fluid dynamics equations was taken as a reference, and following this line of thought the Kerner-Konhäuser (1993, 1994, 1997) model was studied to understand the formation of clusters in highways[9]. It is worth mentioning that it is not the only model which follows this point of view, however it is one of the most studied in the literature as shown in Helbing (1995)[6], Velasco (2005)[18], Méndez (2008)[13], Nagatani (2002)[14] and Zhang (1998)[21]. The main reason for that, is that it can reproduce some well known characteristics of traffic flow and, it is the simplest one to achieve that goal. We notice that some models have been questioned by Daganzo (1995)[2] hence the development of them has overtaken the drawbacks in which they have been involved as showed by Helbing (2008)[7].

In this work we study the macroscopic model known as the Kerner-Konhäuser model which is based in a close analogy with compressible hydrodynamics. The relevant equations considered are the conservation of the number of vehicles in the absence of in/out ramps and a balance equation for the speed. This last equation contains the relaxation of the speed to the so called equilibrium speed given by the fundamental diagram, a viscosity and a kind of hydrostatic pressure measured by the speed variance. It is well known that the set of such equations can be simulated in a closed circuit to study the involved dynamics. The main goal of our work will be the study of solitary traveling waves which are found in the near unstable region. Section 2 presents the model whereas section 3 shows the stability condition and the coexistence curve. In section 4 we give some simulation results and in section 5 we show the guidelines for the construction of the PDE which describes the time evolution of the soliton found in the simulations, lastly in section 6 we give some concluding remarks.

2. THE MODEL

Macroscopic models are useful to understand some characteristics of traffic flow in highways. In the literature there are several models which are based on different grounds. Here we will take the Kerner-Konhäuser model to study the formation of solitary waves. This model considers two coupled equations of motion, one for the density $\rho(x,t)$ which is in fact a conservation equation and the speed

equation $V(x,t)$. This last equation is constructed in close analogy to viscous dynamics of fluids. It contains a term corresponding to the hydrostatic pressure, measured through the velocity variance Θ_0 =constant, and a viscous contribution proportional to a viscosity η_0 =constant. Besides, there is a term describing an average individual relaxation (τ =constant) of the instantaneous speed to the so called equilibrium speed $V_e(\rho)$, which is given through the fundamental diagram. The continuity equation is then written as

$$\frac{\partial \rho}{\partial t} + \frac{\partial}{\partial x}(\rho V) = 0, \tag{1}$$

and the equation of motion

$$\frac{\partial V}{\partial t} + V\frac{\partial V}{\partial x} = -\frac{\Theta_0}{\rho}\frac{\partial \rho}{\partial x} + \frac{\eta_0}{\rho}\frac{\partial^2 V}{\partial x^2} + \frac{1}{\tau}\big[V_e(\rho) - V\big]. \tag{2}$$

The fundamental diagram is taken from the experimental data as described in the literature[9], the maximum density and velocity are also given,

$$\rho_{max} = 140\ veh/km, \qquad V_{max} = 120\ km/h, \tag{3}$$

$$\frac{V_e}{V_{max}} = -3.72\times 10^{-6} + \left[1 + exp\left(\frac{\frac{\rho}{\rho_{max}} - 0.25}{0.06}\right)\right]^{-1}. \tag{4}$$

It is usual to take the velocity variance as $\Theta_0 = (45\ km/h)^2$, the viscosity $\eta_0 = 600\ km/h$ and the relaxation time $\tau = 30\ s$, here we will take several values to see the effect of parameters in speed of the solitary wave which is formed after the transient. The region taken to do the simulations is $x \in [-L, L]$ and $t \in [0, T]$ and we chose periodic boundary conditions for both the density and the speed

$$\rho(-L,t) = \rho(L,t) \qquad V(-L,t) = V(L,t). \tag{5}$$

On the other hand, the initial conditions are taken as a perturbation around the homogeneous steady state specified through the density ρ_e and $V_e(\rho_e)$, in particular we take

$$\rho(x,0) = \rho_e + C_1 cosh^{-2}\left(\frac{x-x_0}{\omega_+}\right) - C_2\frac{\omega_+}{\omega_-}cosh^{-2}\left(\frac{x-x_1}{\omega_-}\right),$$
$$\rho(x,0)\ V(x,0) = \rho_e\ V_e(\rho_e), \tag{6}$$

where the constants $C_1, C_2, \omega_+, \omega_-, x_0, x_1$ will be given for each illustrated case.

3. STABILITY CONDITION

The equations of motion for this model (1)-(2) are nonlinear and coupled, hence the first step in their analysis is given when we realize that the homogeneous steady state characterized with ρ_e, V_e is an exact solution of them. Then as a second step, we consider a linear stability analysis by means of a small perturbation which allows the linearization around the homogeneous steady state. The perturbation is written as

$$\rho(x,t) = \rho_e + \tilde{\rho}\ exp(ikx + \gamma t), \tag{7}$$

$$V(x,t) = V_e + \tilde{V} exp(ikx + \gamma t), \tag{8}$$

where k is the wave vector and the real part of γ will determine if the perturbations will decrease or grow. The direct substitution of the perturbations given in Eqs. (7,8) allows the calculation of eigenvalues in the linearized system, as a result we obtain the speed of propagation of the long wave length perturbation waves

$$c = V_e(\rho_e) + \rho_e V_e'(\rho_e), \tag{9}$$

and the real part of the eigenvalues to the leading orders in the wave vector, namely

$$\Re\gamma_{(+)} = -\tau k^2\left(\Theta_0 - \rho_e^2|V_e'|^2\right) + \mathcal{O}(k^4), \tag{10}$$

$$\Re\gamma_{(-)} = -\frac{1}{\tau} + \mathcal{O}(k^2). \tag{11}$$

In order to obtain stability in the homogeneous steady state the real parts of both eigenvalues must be negative, from Eqs. (10,11) we can see that in the long wavelength regime $\gamma_{(+)}$ gives the stability condition,

$$\rho_e|V_e'| \ < \ \sqrt{\Theta_0}, \tag{12}$$

where $|V_e'|$ is the absolute value of the derivative with respect to the density in the fundamental diagram and, it is evaluated in ρ_e. When the inequality holds true we have stability, otherwise we are in the unstable region. The case where $\rho_e|V_e'| = \sqrt{\Theta_0}$ corresponds to marginal stability. Also, the leading orders in the wave vector for $\Re\gamma_{(+)}$, $\Re\gamma_{(-)}$ as shown in Eqs. (12,13) allow us the identification of two time scales in the problem, making necessary the multiple scales method when we go to the nonlinear problem, see Johnson (2004)[8]. The small parameter measuring this effect is given through the stability condition (12) written in terms of dimensionless quantities. Figure 1 represents the stable and unstable regions according to the fundamental diagram given in Eq. (4), the solid curve gives us the so called coexistence curve, which is constructed taking the marginal stability condition for each value in the density.

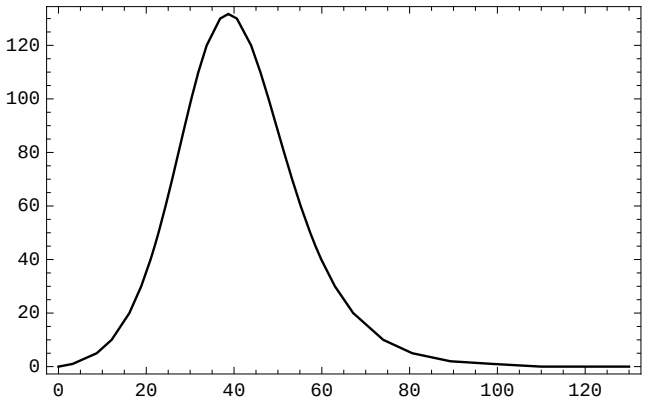

Fig. 1. Stable and unstable regions determined by Eq. (12) and the solid line corresponds to the coexistence curve. Stable regions are outside the coexistence curve, whereas the unstable region is inside it. The vertical axis represents $\sqrt{\Theta_0}$ and in the horizontal axis we have the density ρ_e.

4. SIMULATIONS

The numerical simulations start with the initial and the boundary conditions described in section 2 and we will

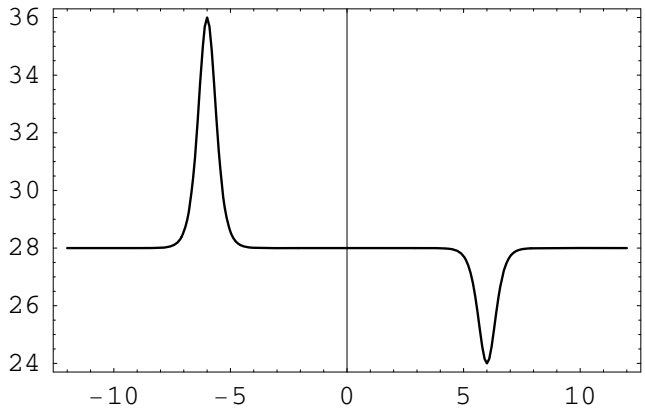

Fig. 2. Initial condition. The vertical axis represents the density ρ (veh/km) and the horizontal axis corresponds to the position x (km). The equilibrium density is $\rho_e = 28$ veh/km.

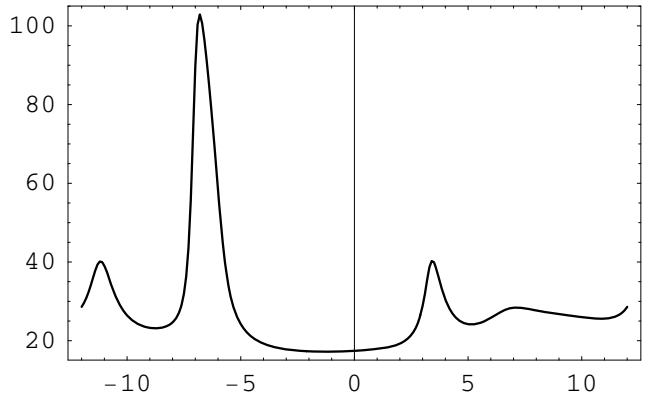

Fig. 3. Density profile as a function of position at $t = 10.0$ min. The vertical axis represents the density ρ (veh/km) and the horizontal axis corresponds to the position x (km).

give 3 examples of the obtained solution. In Figure 2 we consider the length $L = 12.0$ km and two perturbations of different size separated by a distance of 12.0 km, in particular their positions are $x_0 = -6.0$ km and, $x_1 = 6.0$ km respectively. Their width $\omega_+ = \omega_- = 0.5$ km and their amplitudes $C_1 = 8$ veh/km, $C_2 = 4$ veh/km. The equilibrium density around which the perturbation is developing was taken as $\rho_e = 28$ veh/km and, V_e is given through the fundamental diagram (3) and, Figure 2 shows the initial condition ($t = 0.0$ s). In Figure 3 we have the time evolution of the density profile after $t = 10.0$ min in the simulation. This profile corresponds to the transient and it changes until the steady state profile is reached, then it becomes permanent as shown in Figure 4. In this case the final profile represents a soliton which corresponds to a cluster which does not disappear even when the simulation time is long enough.

Its permanence is a remarkable characteristic of a soliton wave and in traffic flow it means that in a closed circuit, a jam will be permanent. We recall that in this case we had two bumps in the initial condition, however the final profile leads to one soliton.

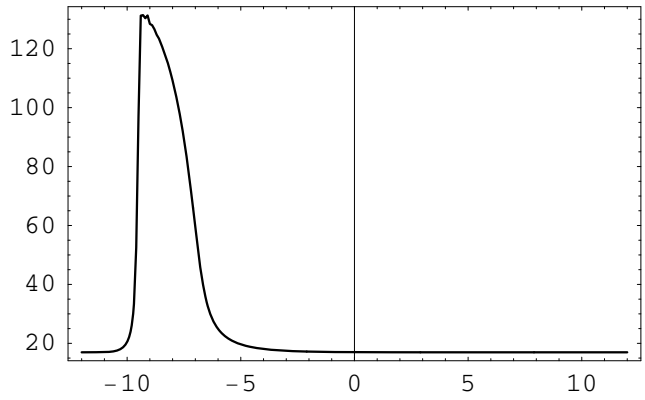

Fig. 4. Density profile as a function of position at $t = 500.0$ min. The vertical axis represents the density ρ (veh/km) and the horizontal axis corresponds to the position x (km).

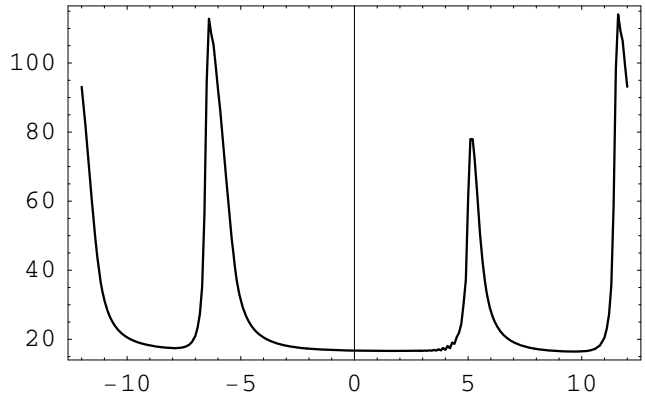

Fig. 5. Density profile as a function of the position at $t = 20$ min. The vertical axis corresponds to the density ρ (veh/km) and the horizontal axis to the position x (km).

In the second example, represented in Figure 5, we have taken equal amplitudes in the initial condition, $C_1 = C_2 = 4$ veh/km, all other parameters are the same as in Figs. 3, 4. In this case the apparition of the soliton is retarded and it is necessary to wait a longer time. The remarkably fact is that in the final stage there are two solitons present, they are equal and their amplitude is essentially the same, as shown in Figure 6 for $t = 490$ min. We notice that the width of solitons in this case is different than the width of the soliton in Figure 4, though both correspond to a final stage of evolution. It means that the initial condition is playing a role in the final profile.

In figure 7 we have taken a longer circuit $L = 24.0$ km, the bumps are originally in $x_0 = -12$ km and $x_1 = 12$ km. They have different amplitudes $C_1 = 8.0$ veh/km, $C_2 = 4.0$ veh/km and the same width $\omega_+ = \omega_- = 0.5$ km. Figure 7 represents an intermediate step in the transient which was taken after $t = 70.0$ min.

Now the time evolution in the density profile changes completely, in the transient we have up to six clusters at $t = 20$ min and only two clusters after $t = 80$ min. In this case the final stage shows two solitary waves which

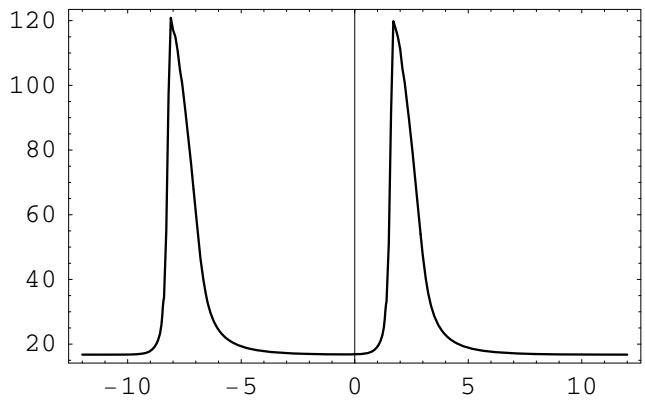

Fig. 6. Density profile as a function of the position at $t = 490\ min$. The vertical axis corresponds to the density ρ (veh/km) and the horizontal axis to the position x (km).

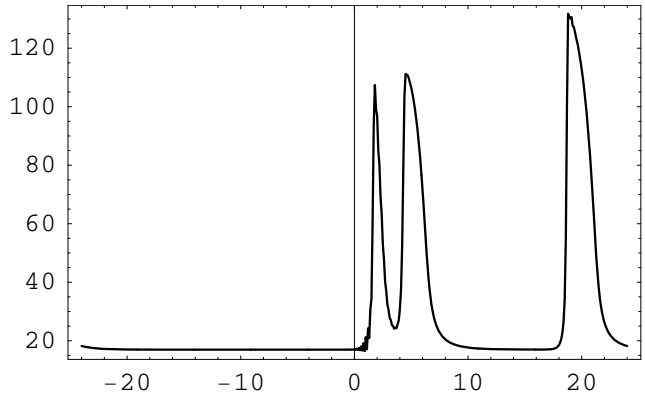

Fig. 7. The density profile as a function of position at $t = 70.0\ min$. Vertical and horizontal axes correspond to the density ρ (veh/km) and position x (km), respectively. The total length of the highway is 48.0 km, the amplitude of bumps in the initial condition are different.

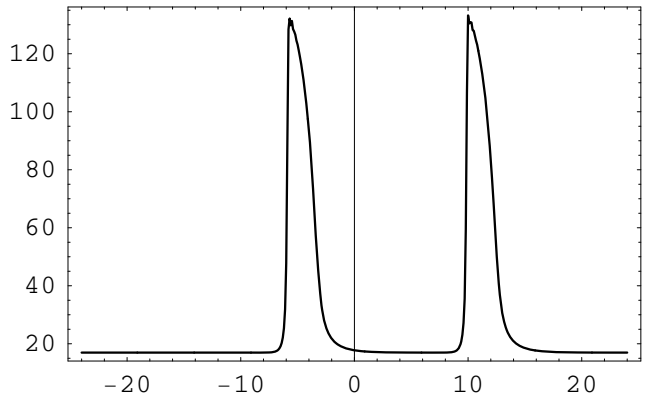

Fig. 8. The density profile as a function of position at $t = 500.0\ min$. Vertical and horizontal axes correspond to the density ρ (veh/km) and position x (km), respectively. The total length of the highway is 48.0 km, the amplitude of bumps in the initial condition are different.

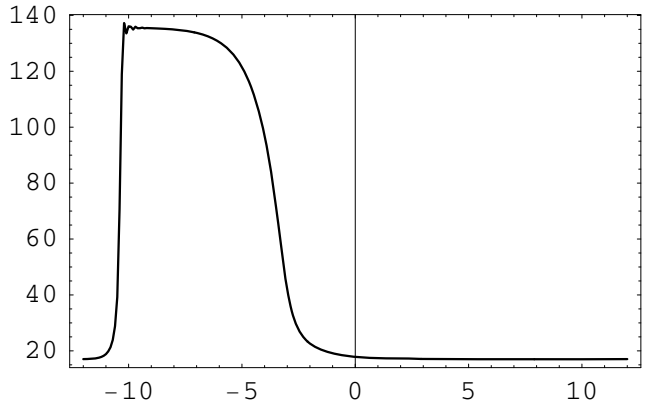

Fig. 9. Density profile as a function of position. The equilibrium density is $\rho_e = 50\ veh/km$.

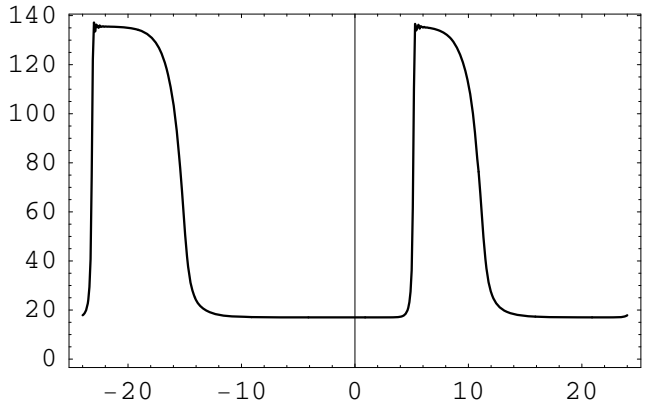

Fig. 10. The density as a function of the position. The equilibrium density is bigger $\rho_e = 50\ veh/km$ and the length of the circuit is $L = 24.0\ km$. The clusters become of different width.

do not interact between themselves, representing a pair of well defined solitons, as shown in Figure 8.

It is important to mention that the Θ_0 parameter plays a very important role in the problem since it determines the stability condition (12). The cases represented in figures 2-8 are located in the unstable region $\rho_e = 28\ veh/km$, $\Theta_0 = (45\ km/h)^2$. On the other hand, when we take a smaller density ρ_e, the initial perturbation dies completely after a relative small simulation time. It means that in the stable region there are not traveling waves. The same effect is observed when the speed variance Θ_0 becomes greater, until the density obtained in the simulation becomes greater than the maximuum density allowed.

In the case where the equilibrium density ρ_e is big enough, we found one soliton formed after the transient, the remarkable fact being that in such a case the width of the solitary wave is bigger. This characteristic can be explained by recalling that the density is a conserved quantity, in a closed circuit without in/out ramps, and a bigger equilibrium density means a bigger number of vehicles in the circuit. Then the final cluster will contain a total number of vehicles bigger than the cases where the equilibrium density is not so big. Figure 9 shows the results for the profile in the density when the equilibrium

density is $\rho_e = 50.0\ veh/km$, $L = 12.0\ km$, the speed variance $\Theta_0 = (45\ km/h)^2$. This case also corresponds to the unstable region.

As a last example we considered the equilibrium density as $\rho_e = 50\ veh/km$ with a circuit in which $L = 24.0\ km$. Now there are two clusters in the final stage but they have different width, the details are shown in Figure 10.

5. FORMAL DESCRIPTION OF THE SOLITON

The traveling wave we have seen in the simulation results can be described as a soliton and to show its presence we have written the equations of motion (1)-(2) in a moving reference frame moving with speed $c_s =$ constant. The systematic development in the small parameter, given by the stability condition, drives to a leading term which can be identified with the Korteweg-de Vries equation (KdV) for the density perturbation $\hat{\rho}(x,t)$. The equations of motion are written in terms of the scaled coordinates and time, as done by Kürtze and Hong (1995)[11]. It should be mentioned that this problem has been studied in the literature with the car-following model, which can also be written as a continuum model with a fundamental diagram depending on the headway distance, see Berg and Woods (2001), [1] Zhu and Dai (2008), [22] Ge *et al* (2005)[4]. In this case the results also show a soliton like behavior in the leading order. In the Kerner-Konhäuser model we are studying here, we can follow a similar procedure to obtain the KdV equation in the nonlinear regime and the analytic solution is given as

$$\hat{\rho} = \frac{3(c_s - c)}{|2V_e' + \rho_e V_e''|} sech^2\left[\sqrt{\frac{\rho_e(c_s - c)}{4\eta_0\tau(c_s - V_e)}}(x - c_s t - z_0)\right].$$

This solution is valid when the amplitude $\frac{3(c_s-c)}{|2V_e'+\rho_e V_e''|} > 0$ in the soliton as well as $\frac{(c-c_s)}{(V_e-c_s)} > 0$, these conditions assure that the density is positive and the soliton width is a real number. The quantity V_e'' is the second derivative with respect to the density in the fundamental diagram, evaluated in ρ_e. On the other hand, z_0 is an integration constant which represents the position of the maximuum density in the traveling wave. The found solution tells us some important details in the soliton. First, we notice that the soliton amplitude is determined essentially by the fundamental diagram, through its derivatives, the propagation speed of long wavelength perturbations and, the speed of the reference frame. Second, the soliton is a symmetric function in the argument and this characteristic is not seen in the numerical simulations where it is clear that the soliton profile is unsymmetrical. Now we define the width of the traveling wave as follows,

$$\Delta = \frac{\int_L^L (z - z_0)^2 \hat{\rho}\, dz}{\int_L^L \hat{\rho}\, dz}, \tag{13}$$

where $z = x - c_s t$. In this case it is clear that z_0 represents the position of the maximum in the soliton density, which is also moving with the velocity c_s. A direct calculation in Eq. (13) gives us that

$$\Delta = 0.822467\delta, \quad \delta = \sqrt{\frac{4\eta_0\tau}{\rho_e}\frac{(V_e - c_s)}{(c - c_s)}}. \tag{14}$$

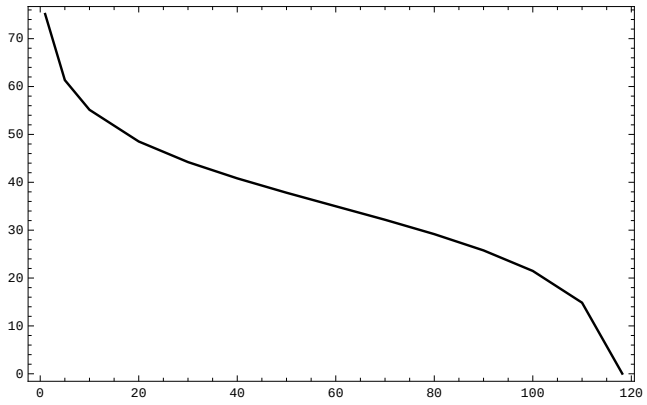

Fig. 11. The curve shows the separation between the regions where it is possible to find the soliton solution. The horizontal axis corresponds to the density ρ_e whereas in the vertical axis we have the c_s value.

Now it is clear that the soliton characteristics depend on the viscosity, the individual relaxation time, the fundamental diagram and, the speed of the reference frame. The result concerning the asymmetric density distribution can be due to the fact that the analytic solution is the leading approximation and, the simulation results include all factors present in the model. It is a future work the search for better approximations to reproduce the asymmetry we can see directly in numerical calculations. Finally in Figure 11, we show the region in the density ρ_e and the speed of the reference frame c_s for which it is possible to obtain the soliton as a solution. Notice that to see the formation of the traveling wave in the small density region (free traffic), the speed of the reference frame must be taken almost as big as the speed given in the fundamental diagram for this value in density. On the other hand, when the density is big enough (congested traffic) the speed c_s necessary to see the soliton reduces. It means that the soliton speed changes according to the density regime in traffic.

6. CONCLUDING REMARKS

In this work we have shown numerically the formation of a solitary wave in a continuum model which is based in a close analogy with compressible fluid dynamics. The simulation results show that after a transient period, the solitary wave is formed and it stays for long simulation times without changes in its structure. The stability in the problem depends on the fundamental diagram and the speed variance. On the other hand, the wave characteristics depend on the model parameters specified through the viscosity, the individual relaxation time, the density around which the perturbation is developed and the speed of the moving reference frame. All calculations we have done are based on a macroscopic model and the traveling wave solution obtained in the simulation is supported by the perturbation analysis. Such an analysis is not exact but contains some approximations which have given us symmetrical waves. Now, we wonder if in the real traffic we can find a soliton structure. So far, this question can be answered qualitatively in a comparison with the experiments done in a closed circuit. There, it has been shown that an initial homogeneous state develops in a well defined cluster of vehicles moving upstream. The cluster does not

change its structure, but evolves along the highway with a constant velocity as found by Sugiyama *et al* (2005, 2008). [19][20] All these facts agree completely with the results we have shown in this work.

REFERENCES

[1] P. Berg, A. Woods. On-ramp simulations and solitary waves of a car-following model. *Phys. Rev. E* 64, 035602, 2001. P. Berg, A. Mason, A. Woods. Continuum approach to car-following models. *Phys. Rev. E* 61, 1056-1066, 2000.

[2] C. F. Daganzo. Requiem for second-order fluid approximations of traffic flows. *Transpn Res. B* 29B, 277-286, 1995.

[3] P. G. Drazin and R. S. Johnson. *Solitons: an Introduction*, Cambridge Univ. Press 1990.

[4] H. X. Ge, R. J. Cheng and S. Q. Dai. KdV and kink-antikink solitons in car-following models. *Physica A* 357, 466-476, 2005.

[5] B. D. Greenshields. In Proc. Highway Res. Board 14, 448, 1935.

[6] D.Helbing. Improved fluid-dynamic model for vehicular traffic. *Phys. Rev. E* 51, 3164-3169, 1995.

[7] D. Helbing. Characteristic speeds faster than the average vehicle speed do not constitute a theoretical inconsistency of macroscopic traffic models. *arXiv:0805.3402v1*, 2008.

[8] R. S. Johnson. *Singular Perturbation Theory*, Springer, 2004.

[9] B. S. Kerner and P. Konhäuser. Cluster effect in initally homogeneous traffic flow. *Phys. Rev. E* 48, R2335-R2338, 1993. B. S. Kerner, P. Konhäuser, Structure and parameters of clusters in traffic flow. *Phys. Rev E* 50, 54-87, 1994. B. S. Kerner and P. Konhäuser. Asymptotic theory of traffic jams. *Phys. Rev. E* 56, 42004216 1997.

[10] R. D. Kühne, R. Beckschulte. In *Transportation and traffic theory*. Editor C. F. Daganzo, Proc. 12th Int. Symp. on Trans. and Traffic Theory, Elsevier, 1993.

[11] D. A. Kürtze and D. C. Hong. Traffic jams, granular flow, and soliton selection. *Phys. Rev. E* 52, 218-221 1995.

[12] M. J. Lighthill and G. B. Whitham. On kinematic waves II: A theory of traffic flow on long crowded roads. *Proc. Royal Soc. London A Math. Phys. Sci.* 229, 317-345, 1955.

[13] A. R. Méndez and R. M. Velasco. An alternative model in traffic flow equations. *Transpn. Res. B* 42, 782-797, 2008.

[14] T. Nagatani. The physics of traffic jams. *Rep. Prog. Phys.* 65, 1331-1386, 2002.

[15] P. Nelson. Synchronized traffic flow from a modified Ligthill-Whitham model. *Phys. Rev. E* 61, R6052-R6055 2000.

[16] H. J. Payne. In *Mathematical Models of Public Systems* Editor. G. A. Bekey 1, 51, 1971.

[17] P. I. Richards. Shock waves on the highway. *Op. Res.* 4, 4251, 1956.

[18] R. M. Velasco and W. Marques Jr. Navier-Stokes-like equations for traffic flow. *Phys. Rev. E* 72, 046102, 2005.

[19] Y. Sugiyama, M. Fukui, M. Kikuchi, K. Hasebe, A. Nakayama, K. Nishinari, S. Tadaki, S. Yukawa. Traffic jams without bottlenecks-experimental evidence for the physical mechanism of the formation of a jam. *New Journal of Physics* 10, 033001, 2008.

[20] Y. Sugiyama, A. Nakayama, M. Fukui, K. Hasebe, M. Kikuchi, K. Nishinari, S. Tadaki, S. Yukawa. Observation, Theory and Experiment for Freeway Traffic as Physics of Many-Body Ssytem. *TGF03* Springer, 2005.

[21] H. M. Zhang, On the consistency of a class of traffic flow models. *Transpn. Res. B* 32, 101-105, 2003.

[22] H. B. Zhu and S. Q. Dai. Numerical simulation of soliton and kink density waves in traffic flow with periodic boundaries. *Physica A*, 387, 4367-4375, 2008.